

A full solution of Brownian motion

Hanqing Zhao^{1,2} and Hong Zhao^{1,*}

¹*Department of Physics and Institute of Theoretical Physics and Astrophysics,
Xiamen University, Xiamen 361005, Fujian, China*

²*Department of Modern Physics, University of Science and Technology of China, Hefei 230026, China*

Brownian motion has served as a pilot of studies in diffusion and other transport phenomena for over a century. It is known that a full description of Brownian motion in the entire course of time should involve both kinetic and hydrodynamic effects. Nevertheless, a formula accounts for both effects has been established only for the limiting case, namely, when Brownian particles are much bigger and heavier than fluid particles. Moreover, for applications it is important to consider small Brownian particles down to a size smaller than fluid particles. But, unfortunately, in these cases only formulae in the short- or long-time limit are available. In this Letter, we derive a general formula for Brownian motion applicable to a wide spectrum of suspended particle, with sizes from being smaller than the fluid particles to comparable to the usual Brownian particles. Our analytical results are well corroborated by the numerical experiments.

Diffusion plays a vital role in various fields [1–3]. For a suspended particle in a fluid, it has been known that its velocity autocorrelation function (VACF) decays exponentially as $C_K(t) = C(0) \exp[-C(0)t/D_0]$ at short times [4–6], followed by a power-law tail $C_H(t) \sim t^{-d/2}$ [7–18], where d is the fluid dimension. The former is a result of the kinetic theory, while the latter is predicted by hydrodynamics. The hydrodynamic effect may play a non-negligible role even in short times. To get an accurate evaluation of the hydrodynamic effect, by which one can separate the kinetic and hydrodynamic contributions, we need a full expression of the VACF applicable in the entire course of time. Such an expression has been found by the generalized Langevin equation approach based on the fluctuating hydrodynamics [6, 16, 17]. However, it is applicable only for Brownian particles much heavier and bigger than the fluid particles and in three dimension (3D). For light Brownian particles this formula leads to an unphysical consequence as $t \rightarrow 0$ [6]. In recent years, two-dimensional (2D) fluids have become of practical importance, e.g., 2D water confined by graphene flakes [19, 20], quark-gluon plasma under certain conditions [21], cell membranes and other kind of biomembranes, and so on. The lack of a 2D full formula thus turns out to be a serious issue. An additional important reason is that, for applications, one may encounter suspended particles of various sizes, and the diffusion of small particles are of particular interests. For small-molecule drugs [22, 23], small drug molecules are preferred as they diffuse faster.

On the other hand, the state-of-the-art technologies have made accurate measurements of instantaneous position and even velocity of individual molecules within the experimental reach [24–31]. Owing to this, in recent years there has been a renewal of experimental interests in examining the particle diffusion theory [27, 28, 32–35]. A very focus is to probe diffusion anomalies of hydrody-

dynamic origin [27, 32, 33, 35]. As such, a general formula of Brownian motion, that can clearly distinguish the kinetic and hydrodynamic contributions, becomes urgently important.

The purpose of this work is to derive a general formula for particle diffusion that meets these requirements. We start with the framework of the generalized hydrodynamics [36, 37] suggesting that, by replacing the diffusion constant with a time-dependent diffusion coefficient $D(t)$, a particle diffuses following the density distribution $\rho(\mathbf{r}, t) = \frac{1}{4\pi D(t)t} \exp[-\frac{r^2}{4D(t)t}]$, when the hydrodynamic effect is taken into account. $D(t)$ is connected to the VACF by

$$D(t) = \int_0^t C(t') dt', \quad (1)$$

which gives the usual Green-Kubo formula at $t \rightarrow \infty$.

Let us consider a tagged Brownian particle of mass M . Without loss of generality, we assume that initially it is located at the origin and moves along the x -axis with a momentum $\mathbf{p}(0) \equiv [p_x(0), 0, 0]$. The VACF is $C(t) = \langle p_x(t)p_x(0) \rangle / M^2$, where $\langle \cdot \rangle$ represents the ensemble average. The instant momentum of the tagged particle can be decomposed into three parts, dubbed the kinetic, hydrodynamic and random part, respectively: $p_x(t) = p_x^K(t) + p_x^H(t) + p_x^R(t)$. The kinetic part, $p_x^K(t)$, is the portion of $p_x(0)$ that remains at time t ; The hydrodynamic part, $p_x^H(t)$, is the portion that is transferred back to the tagged particle through surrounding particles. The random part, $p_x^R(t)$, comes from random collisions with other particles, which is uncorrelated with $p_x(0)$. Taking these into account, we have

$$C(t) = C_K(t) + C_H(t). \quad (2)$$

By the kinetic theory, $p_x^K(t) = p_x(0) \exp[-\frac{C(0)}{D_0}t]$, which gives $C_K(t)$ straightforwardly, our task is thus to calculate $p_x^H(t)$ to obtain $C_H(t)$. Note that at time t , the portion of momentum $p_x(0)$ that has been transferred into fluid in the kinetic process is $p(0)[1 - \exp(-\frac{C(0)}{D_0}t)]$. Denote by $p(\mathbf{r}, t)$ its density, i.e., the momentum transferred

* zhaoh@xmu.edu.cn

to a unit volume at position \mathbf{r} and time t , then a particle at \mathbf{r} and time t has an average velocity $p(\mathbf{r}, t)/\rho$, which gives the velocity field of vortex backflow triggered by the tagged particle. Here ρ is the fluid density. The tagged particle, irrespective of its shape and mass, has the same velocity on average because it is driven by the backflow. This is equivalent to the general assumption that local equilibrium can be established rapidly [38]. Nevertheless, the transferred momentum can not establish the backflow promptly. To determine the time after which the backflow sets in, we introduce a function $R(t)$ to characterize the retarded effect in response. It leads to

$$p_x^H(t) = \frac{M}{\rho} (1 - e^{-\frac{C(0)}{D_0}t}) R(t) \int p(\mathbf{r}, t) \rho(\mathbf{r}, t) d\mathbf{r}, \quad (3)$$

where $\rho(\mathbf{r}, t)$ is the probability for the tagged particle to appear in a unit volume at position \mathbf{r} and time t .

We next calculate $p_x(\mathbf{r}, t)$. It follows the hydrodynamic equations that arise from the conservation laws of the particle number, energy, and momentum. We first linearize these equations and perform the Fourier (Laplace) transformation with respect to space (time), which is a conventional procedure [38]. The key difference of our treatments from others is that we apply the δ type initial conditions to be $\mathbf{p}(\mathbf{r}, t=0) = [p_x(0)\delta(\mathbf{r}), 0, 0]$, $\Delta T(\mathbf{r}, t=0) = \Delta T\delta(\mathbf{r})$, and $\Delta n(\mathbf{r}, t=0) = \Delta n\delta(\mathbf{r})$, where $\Delta T(\mathbf{r}, t)$ and $\Delta n(\mathbf{r}, t)$ are the temperature and particle density fluctuations, respectively. It is precisely due to this initial condition that the 5×5 hydrodynamic matrix is reduced to a 3×3 one, and subsequent analytical derivations are substantially simplified. Solving the hydrodynamic equations (see Supplementary Materials [39], section S1), we obtain $p_x(\mathbf{k}, t) = p_x^V(\mathbf{k}, t) + p_x^S(\mathbf{k}, t)$ in the Fourier space under the long wave approximation, where

$$\frac{p_x^V(\mathbf{k}, t)}{p_x(0)} = \frac{k_y^2 + k_z^2}{k^2} \exp(-\nu_0 k^2 t) \quad (4)$$

is the contribution of the shear viscosity mode and

$$\frac{p_x^S(\mathbf{k}, t)}{p_x(0)} = \frac{k_x^2}{k^2} \exp(-\Gamma k^2 t) \cos(c_s k t) \quad (5)$$

is that of the sound mode. Here \mathbf{k} is the wave number, ν_0 is the viscosity diffusivity, c_s the sound speed and Γ the sound attenuation coefficient. Note that they apply to a two-dimensional system as well for which $k_z = 0$. Equation (4) gives the x -component of the vortex backflow triggered by a momentum impulse along the x -axis. The y - and z -component can also be obtained by hydrodynamics, but it is not necessary for calculating the VACF. Difference from previous solutions [9, 38], these solutions are anisotropic, as a consequence of applying the directed impulse momentum to be the initial condition, implying that the profile of backflow triggered by a directed momentum impulse is anisotropic.

To get $C_H(t)$ next, we employ the Parseval formula to transform the spatial integral into a wave-vector integral,

i.e., $\int p_x(\mathbf{r}, t) \rho(\mathbf{r}, t) d\mathbf{r} = (\frac{1}{2\pi})^d \int p_x(\mathbf{k}, t) \rho(\mathbf{k}, t) d\mathbf{k}$, where $\rho(\mathbf{k}, t) = \exp\{-[D_H(t) + D_0]k^2 t\}$. It gives that

$$\frac{C_H(t)}{C(0)} = \frac{M(d-1)}{\rho d} (1 - e^{-\frac{C(0)}{D_0}t}) R(t) [4\pi(D_H(t) + D_0 + \nu_0)t]^{-\frac{d}{2}}, \quad (6)$$

where we have neglected the contribution of sound mode as usually adopted [6, 11, 38]. (The sound mode may result in a small, negligible usually, correction to the VACF. See Supplementary Materials [39], section S2.) Inserting $C_K(t)$ into Eq. (1), we have $D(t) = D_0[1 - \exp(-C(0)t/D_0)] + D_H(t)$, with

$$D_H(t) = \int_0^t C_H(t') dt'. \quad (7)$$

Solving these two coupled equations, we obtain that

$$\frac{C_H(t)}{C(0)} = \frac{M(d-1)}{\rho d} (1 - e^{-\frac{C(0)}{D_0}t}) R(t) (4\pi t)^{-\frac{d}{2}} A^{-\frac{d}{d+2}}, \quad (8)$$

$$D_H(t) = A^{\frac{2}{d+2}} - (D_0 + \nu_0), \quad (9)$$

with

$$A = (D_0 + \nu_0)^{\frac{d+2}{2}} + \frac{M(d-1)(d+2)}{2\rho d} (4\pi)^{-\frac{d}{2}} C(0) \int_0^t (1 - e^{-\frac{C(0)}{D_0}t'}) R(t') t'^{-\frac{d}{2}} dt'. \quad (10)$$

To find the first order correction of $R(t)$, we note that the recovery of momentum memory takes place after a ring collision [9]. The lowest order rings involve three collision events. This process defines the time threshold at which the backflow begins to play a role. The free time obeys the Gamma distribution, i.e., $\frac{1}{\tau} \exp(-t/\tau)$, where τ is the mean free time. Since $R(t)$ is the probability for the memory recovery to occur, it is the joint probability for three independent collision events to occur. This gives

$$R(t) = 1 - \frac{\tau_B^2 e^{-\frac{t}{\tau_B}} - (2\tau_B\tau_F - \tau_F^2 + (\tau_B - \tau_F)t) e^{-\frac{t}{\tau_F}}}{(\tau_F - \tau_B)^2} \quad (11)$$

where τ_B is the mean inverse frequency of the Brownian particle-fluid particle collisions, and τ_F is that of collisions between fluid particles.

Our result Eq. (8) is consistent with the standard kinetic theory at $t \rightarrow 0$, i.e., $C(t) \approx C_K(t)$ at short times. In contrast, the previous result by the generalized Langevin equation fails in this limit [6, 16, 17]: it leads to $C(t \rightarrow 0) = \frac{k_B T}{M_*}$ with $M_* = M + \frac{1}{12} \pi \sigma^3 \rho$, which should be $C(t \rightarrow 0) = \frac{k_B T}{M}$ according to the equipartition theorem. Here k_B is the Boltzmann constant and T the temperature. This is known as an unphysical consequence induced by the incompressibility condition adopted. Only for $\rho/\rho_B \ll 1$ (ρ_B is the density of the Brownian particles), $M_* \sim M$, it approaches the kinetic result; but for

$\rho/\rho_B \sim 1$, as a pollen in water, the canonical Brownian motion, a significant deviation arises: $C(t \rightarrow 0) = \frac{2}{3} \frac{k_B T}{M}$, which remarkably violates the equipartition theorem. As a consequence, $C(t)$ is smaller than that of the kinetic prediction for $t \approx 0$, leading to a significant underestimation of the diffusion coefficient (See Supplementary Materials [39], section S6).

At long-time limit, for $d = 2$, Eq. (8) and (9) give the asymptotic solution that $C_H(t) = C(0) \sqrt{\frac{M}{16\pi\rho}} (t\sqrt{\ln t})^{-1}$ and $D_H(t) = C(0) \sqrt{\frac{M \ln t}{4\pi\rho}}$. They are in agreement with the results obtained by the self-consistent mode coupling approach [40], but contradictory to the $\sim t^{-1}$ law predicted by the traditional hydrodynamic approach. To understand this discrepancy, we see from Eq. (8) that the asymptotic solutions apply for $t \gg t_c \equiv \exp[4\pi\rho M (\frac{D_0 + \nu_0}{k_B T})^2]$, when $(D_0 + \nu_0)$ is much smaller than $D_H(t)$. For sufficiently large t but smaller than t_c , when hydrodynamic contributions have dominated already, i.e., $[1 - \exp(-\frac{C(0)}{D_0}t)]R(t) \sim 1$, but $D_H(t)$ is still negligible, the $\sim t^{-1}$ behavior shows up. That is, the $\sim t^{-1}$ behavior appears in intermediate time, and crosses over to $\sim (t\sqrt{\ln t})^{-1}$ behavior at t_c . Therefore, Eq. (8) unifies the traditional hydrodynamic and self-consistent mode coupling approaches. For $d = 3$, our result is $C(t)/C(0) \sim \frac{2}{3} \frac{M}{\rho} [4\pi(D_0 + \nu_0 + D_H(\infty))t]^{-\frac{3}{2}}$ at long-time limit. Here $D_H(\infty)$ is the saturation value of $D_H(t)$. $D_H(\infty) = [(D_0 + \nu_0)^{\frac{5}{2}} + 0.12 \frac{k_B T}{\pi\rho} (\frac{C(0)}{D_0})^{\frac{1}{2}}]^{\frac{2}{3}} - (D_0 + \nu_0)$ for a fluid particle ($M = m$). This asymptotic behavior differs from previous predictions. Indeed, for the fluid particle, hydrodynamic approaches [7, 9] have predicted that $\frac{C(t)}{C(0)} \sim \frac{2}{3} \frac{M}{\rho} [4\pi(D_0 + \nu_0)t]^{-\frac{3}{2}}$, while for the Brownian particle, the generalized Langevin equation approach has suggested that $\frac{C(t)}{C(0)} \sim \frac{2}{3} \frac{M_*}{\rho} (4\pi\nu_0 t)^{-\frac{3}{2}}$ [6]. The former corresponds to the neglecting of $D_H(\infty)$ in our results, and the latter deviates significantly from ours where there is no room for D_0 and M being replaced by the effective mass M_* . Therefore, the previous results at long-time limit are approximations of ours (See Supplementary Materials [39], section S6).

Numerical simulation of a 3D fluid for our aim here is still challenging with available computing resources, as a sufficient large system is needed to reveal the long-time tail without being influenced by the finite-size effect. We therefore turn to the 2D hard-disk fluid model to test our results. It consists of N disks of unit mass moving in a square box of size L with the periodic boundary conditions. Considering that the simulation results are free from finite-size effect for $t < L/(2c_s)$ [41], we set $L = 2000$ (see Supplementary Materials [39], section S3). The particle number $N = 40000$, corresponding to an average disk number density $n = 0.01$. The packing density $\phi = n\pi\sigma^2/4$, with σ being the disk diameter. The system's behavior at $2 \leq \sigma \leq 9$, which covers from the gas to the liquid regime, are studied in great details. Note that for this model the crystallization density is $\phi = 0.71$,

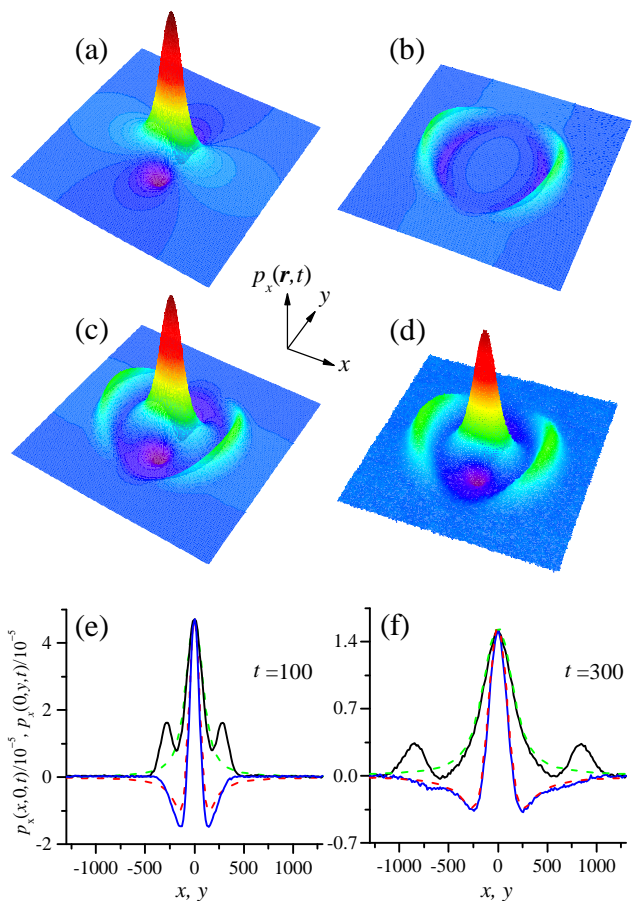


FIG. 1. The hydrodynamic modes. The analytical results for the viscosity mode (a), the sound mode (b), and their superposition (c) at $t = 300$ for $\nu_0 = 8.0$. (d) The simulated $p_x(\mathbf{r}, t)$ at $t = 300$; (e) and (f): The intersections of the simulated $p_x(\mathbf{r}, t)$ with $y = 0$ (black solid lines) and $x = 0$ (blue solid lines) at $t = 100$ and 300 , respectively. They are compared with the viscosity mode given by Eq. (12) with the best fitting value of $\nu_0 = 8.0$. The intersections of the profiles thereby obtained with $y = 0$ ($x = 0$) are represented by the green dashed (red dashed) lines. For simulations $\sigma = 6$.

corresponding to $\sigma = 9.5$. We simulate the system by the event-driven algorithm. The rescaled temperature $T = 1$ (k_B is set to be unity).

The VACF is only governed by the kinetic parameters ν_0 , D_0 , and τ , which can be obtained analytically for fluid particles by the Enskog formula [38, 42]. However, though a lot of efforts have been devoted to numerically testing the Enskog formula, its accuracy is still to be verified. In the following we will compute these parameters by both the Enskog formula and direct simulations.

To measure ν_0 numerically, we note that the viscosity mode, the inverse Fourier transform of Eq. (3), is

$$\frac{p_x^V(\mathbf{r}, t)}{p_x(0)} = \frac{x^2 - y^2}{2\pi r^4} (1 - e^{-\frac{x^2}{4\nu_0 t}}) + \frac{y^2}{4\pi r^2 \nu_0 t} e^{-\frac{x^2}{4\nu_0 t}}. \quad (12)$$

The sound mode can be obtained by numerically per-

$\sigma(\phi)$	2(0.03)	4(0.13)	6(0.28)	8(0.50)	9(0.63)
$\nu_0(\text{E})$	14.1	7.7	6.3	8.5	14.3
$\nu_0(\text{S})$	14.3 ± 0.05	8.3 ± 0.05	8.0 ± 0.05	15.0 ± 1.0	35.0 ± 2.0
$D_0(\text{E})$	13.40	5.70	2.76	1.10	0.59
$D_0(\text{S})$	13.35 ± 0.02	5.68 ± 0.02	2.76 ± 0.02	1.14 ± 0.02	0.66 ± 0.02
$\tau(\text{S})$	13.24 ± 0.03	5.64 ± 0.03	2.76 ± 0.03	1.14 ± 0.03	0.65 ± 0.03

TABLE I. Kinetic coefficients obtained by the Enskog formula (E) and by simulations (S).

forming the inverse transform of Eq. (4). Combining them together leads to a theoretical prediction for $p_x(\mathbf{r}, t)$. As shown in Fig. 1(a)-(c), $p_x(\mathbf{r}, t)$ is anisotropic. Note that Eq. (12) gives the x -component of velocity field of vortex backflow. The y -component of velocity field can also be obtained similarly. Therefore, the viscosity mode gives the analytical solution of the conventional vortex backflow.

Numerically, $p_x(\mathbf{r}, t)$ is computed by the correlation function $\langle \tilde{p}_x(\mathbf{r}, t)p_x(0) \rangle$, i.e.,

$$\frac{p_x(\mathbf{r}, t)}{p_x(0)} = \frac{\langle \tilde{p}_x(\mathbf{r}, t)p_x(0) \rangle - \langle \tilde{p}_x(\mathbf{r} \neq 0, 0)p_x(0) \rangle}{\langle |p_x(0)|^2 \rangle}. \quad (13)$$

Here $\tilde{p}_x(\mathbf{r}, t)$ represents the x -component of the instantaneous momentum density. The result is shown in Fig. 1(d), which confirms the theoretical prediction.

The explicit expression of the viscosity mode allows us to compute ν_0 based on the simulated $p_x(\mathbf{r}, t)$. Specifically, we fit the viscosity mode, i.e., the center peak of the simulated $p_x(\mathbf{r}, t)$, by $p_x^V(\mathbf{r}, t)$. In this way we find $\nu_0 = 8.0$ for $\sigma = 6$. Note that this value is independent of time [c.f. Fig. 1(e)-(f)], implying that hydrodynamics is harmless to the viscosity diffusivity. Previous numerical studies based on the Einstein-Helfand formula have shown that the viscosity diffusivity is independent of the system size either [42], consistent with our findings here. In Table 1 we summarize the value of ν_0 computed for various packing densities (the state equation used in the Enskog formula is the Henderson expression). It is important to note that the result is close to that given by the Enskog formula under the first Sonine polynomial approximation [42] in the dilute gas regime, but the discrepancy between them becomes significant as the packing density increases. This result supports the usual belief that the Enskog formula is accurate only at low densities [41].

We measure D_0 by fitting the simulated VACF with $C_K(t)$ at $t \rightarrow 0$. We emphasize that the time window for fitting must be sufficiently narrow to ensure that the hydrodynamic effect does not play a role yet (see Supplementary Materials [39], section S4). We discard the well-known method by the mean-squared displacement, i.e., $\langle r^2(t) \rangle = 2dD_0t$, where one has to fit D_0 at $t > t_\tau$ that, at such a time scale, the hydrodynamic contribution may have significantly influenced the fitting (see Supplementary Materials [39], section S5). The results for a fluid particle are given in Table 1. As a comparison, the D_0

values obtained by the Enskog formula are given in Table 1 as well: It can be seen that the agreement between them is excellent for almost all densities: the discrepancy is less than 10% even for the highest density ($\sigma = 9$) studied in simulations. For the diffusion constant D_0 , contrary to the common belief that the Enskog formula is only accurate at low densities, our results suggest that it is valid at a much broader regime, if we interpret it as the pure kinetic part of the diffusion coefficient. In fact, by employing the relation between the mean free time τ and the kinetic diffusion constant [38], i.e., $D_0 = \frac{C(0)d}{2}\tau$, we can calculate D_0 in the third way. In a 2D fluid, it appears $D_0 = \tau$ with dimensionless unity. The parameter τ can be easily measured in simulations, and the result is given in Table 1. The mean free time is determined only by the first collision between tagged particle and fluid particles, in which case there is no memory feedback taking place. It thus describes the pure kinetic effect. The results are in perfect agreement with that by fitting the short-time behavior of the VACF, confirming again the validity of the latter.

With D_0 , ν_0 and τ at hand, we can calculate $C(t)$ and $D(t)$. Figure 2(a)-(e) show the VACF for a fluid particle at different packing densities, Fig. 2(f)-(h) are for a Brownian particle of unit mass with different diameters, and Fig. 2(i)-(j) are for a Brownian particle of the fixed diameter but different masses. We see that in most cases Eq. (7) is in excellent agreement with the simulation results. A slight discrepancy between theoretical and numerical results appears in certain extreme conditions, as in Fig. 2(e) and (h). For example, In Fig. 2(e) the fluid density is so high that it is very close to the crystallization point that the system may have deviated from the fluid structure to certain extent. Fig. 2(h) is for a Brownian particle with $\rho/\rho_B \sim 5.8$, whose density is much smaller than the fluid. These extreme situations have been far beyond the usual scope of Brownian motion. In spite of this fact, it is encouraging that the deviation in the diffusion coefficient is negligible (see Supplementary Materials [39], section S6).

In summary, we have derived a general formula for Brownian motion, applicable to a broad spectrum of Brownian particles regardless of their shapes and sizes (if the rotation is ignored); the result applies to very general environments, ranging from dilute gases to dense liquids. This result allows us to describe the kinetic-hydrodynamic crossover of the VACF, leading to an ac-

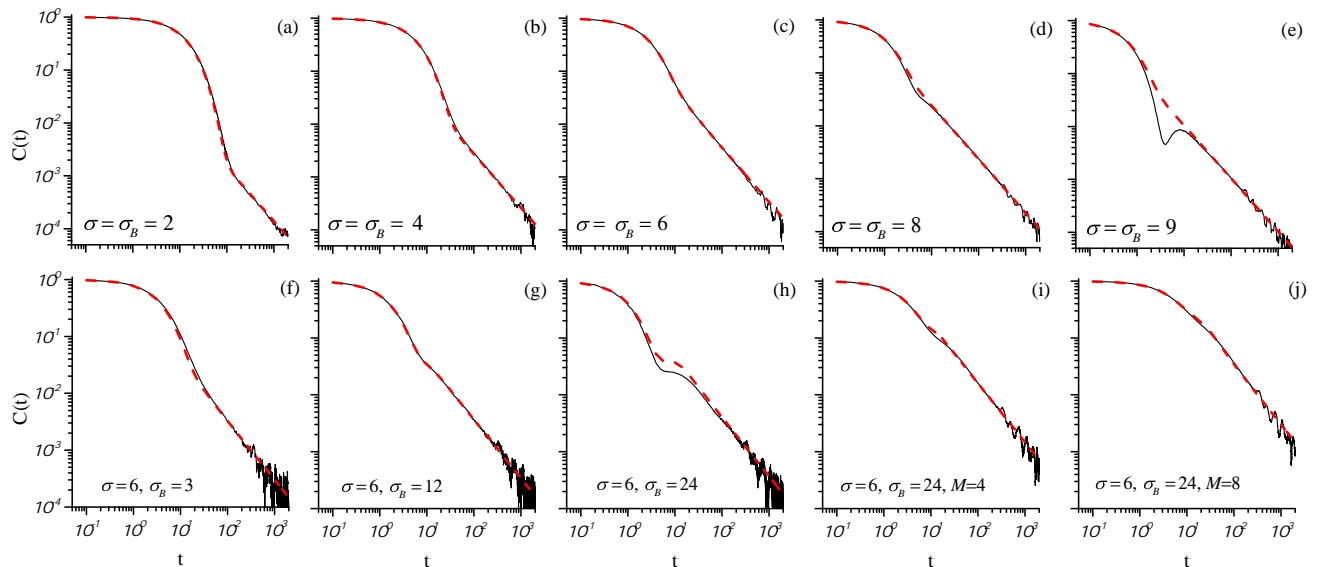


FIG. 2. Comparison of the analytical (red dashed line) and the numerical (black solid line) result of the VACF. For (a)-(h), the mass of the Brownian particles is set to be unity, the same as the fluid particles. In (a)-(e), the diameter of the Brownian particles σ_B is the same as the fluid particles as well, and in (f)-(h), $\sigma_B=3, 12$, and 24 , respectively. (i)-(j) are for a Brownian particles with diameter $\sigma_B=24$ and mass $M=4$ and 8 , respectively. The parameters ν_0 and D_0 for fluid particles are given in Table 1. D_0 for Brownian particles in (f)-(j) is obtained by fitting the simulated VACF around $t=0$ (see text) which gives $D_0=3.85, 1.70, 1.1, 0.85$, and 0.80 , respectively.

curate account of both the kinetic and hydrodynamic contributions to the diffusion coefficient. For 3D fluid, the formula of generalized Langevin equation approach is a crude approximation of ours and fails to quantitatively calculate the diffusion coefficient for light particles, whereas our formula indicates that the hydrodynamic contribution can reach the order of the kinetic diffusion constant. For 2D cases, our formula gives, for the first time, the full expression of the diffusion coefficient, which indicates that the hydrodynamic effect may dominate.

The present study also indicates an accurate way to measure the kinetic diffusion constant and the viscosity diffusivity. For the former, we fit the VACF with $C_K(t)$ at a time range much smaller than the mean free time to avoid the hydrodynamic influence. For the latter, the analytical solution of the viscosity mode triggered by a directed momentum impulse is obtained, and in turn, the viscosity diffusivity is obtained by fitting the spatio-temporal correlation of the momentum fluctuation. With the accurately measured kinetic parameters, we found that the Enskog formula is very accurate for D_0 , but for the viscosity diffusivity, applicable only at low densities.

We are grateful to J. Wang and C. Tian for useful discussions. This work is supported by the NSFC (Grants No. 11335006).

-
- [1] Y. Pomeau and P. Resibois. Time dependent correlation functions and mode-mode coupling theories. *Physics Reports*, 19(2):63–139, 1975.
 - [2] P. Hänggi and F. Marchesoni. 100 years of brownian motion. *Chaos*, 15(2), 2005.
 - [3] X. Bian, C. Kim, and G. E. Karniadakis. 111 years of brownian motion. *Soft Matter*, 12(30):6331–6346, 2016.
 - [4] A. Einstein. Un the movement of small particles suspended in stationary liquids required by the molecular-kinetic theory of heat. *Annalen der Physik*, 17:549–560, 1905.
 - [5] G. E. Uhlenbeck and L. S. Ornstein. On the theory of the brownian motion. *Physical review*, 36(5):823, 1930.
 - [6] E. H. Hauge and A. Martin-Löf. Fluctuating hydrodynamics and brownian motion. *Journal of Statistical Physics*, 7(3):259–281, 1973.
 - [7] B. J. Alder and T. E. Wainwright. Velocity autocorrelations for hard spheres. *Physical review letters*, 18(23):988, 1967.
 - [8] B. J. Alder and T. E. Wainwright. Decay of the velocity autocorrelation function. *Physical review A*, 1(1):18, 1970.
 - [9] J. R. Dorfman and E. G. D. Cohen. Velocity-correlation functions in two and three dimensions: Low density. *Physical Review A*, 6(2):776, 1972.
 - [10] J. R. Dorfman and E. G. D. Cohen. Velocity correlation functions in two and three dimensions. *Physical Review Letters*, 25(18):1257, 1970.
 - [11] M. H. Ernst, E. H. Hauge, and J. M. J. Van Leeuwen. Asymptotic time behavior of correlation functions. i. ki-

- netic terms. *Physical Review A*, 4(5):2055, 1971.
- [12] M. H. Ernst, E. H. Hauge, and J. M. J. Van Leeuwen. Asymptotic time behavior of correlation functions. ii. kinetic and potential terms. *Journal of Statistical Physics*, 15(1):7–22, 1976.
- [13] R. Zwanzig and M. Bixon. Hydrodynamic theory of the velocity correlation function. *Physical Review A*, 2(5):2005, 1970.
- [14] A. Widom. Velocity fluctuations of a hard-core brownian particle. *Physical Review A*, 3(4):1394, 1971.
- [15] E. J. Hinch. Application of the langevin equation to fluid suspensions. *Journal of Fluid Mechanics*, 72(03):499–511, 1975.
- [16] R. Zwanzig and M. Bixon. Compressibility effects in the hydrodynamic theory of brownian motion. *Journal of Fluid Mechanics*, 69(1):21–25, 1975.
- [17] W. B. Russel. Brownian motion of small particles suspended in liquids. *Annual Review of Fluid Mechanics*, 13(1):425–455, 1981.
- [18] D. Lesnicki, R. Vuilleumier, A. Carof, and B. Rotenberg. Molecular hydrodynamics from memory kernels. *Physical Review Letters*, 116:147804, Apr 2016.
- [19] L. Chen, G. Shi, J. Shen, B. Peng, B. Zhang, Y. Wang, F. Bian, J. Wang, D. Li, and Z. et al. Qian. Ion sieving in graphene oxide membranes via cationic control of interlayer spacing. *Nature*, 2017.
- [20] S. Homaeigohar and M. Elbahri. Graphene membranes for water desalination. *NPG Asia Materials*, 9(8):e427, 2017.
- [21] E. Shuryak. Strongly coupled quark-gluon plasma in heavy ion collisions. *Reviews of Modern Physics*, 89(3):035001, 2017.
- [22] T. K. Warren, R. Jordan, M. K. Lo, A. S. Ray, R. L. Mackman, V. Soloveva, D. Siegel, M. Perron, R. Bannister, and H. C. et al. Hui. Therapeutic efficacy of the small molecule gs-5734 against ebola virus in rhesus monkeys. *Nature*, 531(7594):381–385, 2016.
- [23] M. Xu, E. M. Lee, Z. Wen, Y. Cheng, W. Huang, X. Qian, TCW Julia, J. Kouznetsova, S. C. Ogden, and C. et al. Hammack. Identification of small-molecule inhibitors of zika virus infection and induced neural cell death via a drug repurposing screen. *Nature medicine*, 22(10):1101–1107, 2016.
- [24] H. Craighead. Future lab-on-a-chip technologies for interrogating individual molecules. *Nature*, 442(7101):387–393, 2006.
- [25] C. Di Rienzo, V. Piazza, E. Gratton, F. Beltram, and F. Cardarelli. Probing short-range protein brownian motion in the cytoplasm of living cells. *Nature communications*, 5, 2014.
- [26] C. D. S. Brites, X. Xie, M. L. Debasu, X. Qin, R. Chen, W. Huang, J. Rocha, X. Liu, and L. D. Carlos. Instantaneous ballistic velocity of suspended brownian nanocrystals measured by upconversion nanothermometry. *Nature Nanotechnology*, 11(10):851–856, 2016.
- [27] R. Huang, I. Chavez, K. M. Taute, B. Lukić, S. Jeney, M. G. Raizen, and E. L. Florin. Direct observation of the full transition from ballistic to diffusive brownian motion in a liquid. *Nature Physics*, 7(7):576–580, 2011.
- [28] T. Li, S. Kheifets, D. Medellin, and M. G. Raizen. Measurement of the instantaneous velocity of a brownian particle. *Science*, 328(5986):1673–1675, 2010.
- [29] S. Kheifets, A. Simha, K. Melin, T. Li, and M. G. Raizen. Observation of brownian motion in liquids at short times: instantaneous velocity and memory loss. *science*, 343(6178):1493–1496, 2014.
- [30] M. Hohmann, F. Kindermann, T. Lausch, D. Mayer, F. Schmidt, E. Lutz, and A. Widera. Individual tracer atoms in an ultracold dilute gas. *Physical Review Letters*, 118:263401, Jun 2017.
- [31] Johannes Möller and Theyencheri Narayanan. Velocity fluctuations in sedimenting brownian particles. *Physical Review Letters*, 118:198001, May 2017.
- [32] J. Brillo, A. I. Pommrich, and A. Meyer. Relation between self-diffusion and viscosity in dense liquids: New experimental results from electrostatic levitation. *Physical review letters*, 107(16):165902, 2011.
- [33] B. Lukić, S. Jeney, C. Tischer, A. J. Kulik, L. Forró, and E. L. Florin. Direct observation of nondiffusive motion of a brownian particle. *Physical review letters*, 95(16):160601, 2005.
- [34] A. Jannasch, M. Mahamdeh, and E. Schäffer. Inertial effects of a small brownian particle cause a colored power spectral density of thermal noise. *Physical review letters*, 107(22):228301, 2011.
- [35] T. Franosch, M. Grimm, M. Belushkin, F. M. Mor, G. Foffi, L. Forro, and S. Jeney. Resonances arising from hydrodynamic memory in brownian motion. *Nature*, 478(7367):85–88, 2011.
- [36] W. E. Alley and B. J. Alder. Modification of fick’s law. *Physical Review Letters*, 43(10):653, 1979.
- [37] B. J. Alder and W. E. Alley. Generalized hydrodynamics. *Physics Today*, 37(1):56–63, 1984.
- [38] J. P. Hansen and I. R. McDonald. *Theory of Simple Liquids*. Academic Press, 2006.
- [39] Supplementary materials.
- [40] T. E. Wainwright, B. J. Alder, and D. M. Gass. Decay of time correlations in two dimensions. *Physical Review A*, 4(1):233, 1971.
- [41] M. Isobe. Long-time tail of the velocity autocorrelation function in a two-dimensional moderately dense hard-disk fluid. *Physical Review E*, 77(2):021201, 2008.
- [42] R. García-Rojo, S. Luding, and J. J. Brey. Transport coefficients for dense hard-disk systems. *Physical Review E*, 74(6):061305, 2006.